American Mineralogist, Volume 63, pages 1166–1174, 1978

Manganochromite, palladium antimonide, and some unusual mineral associations at the Nairne pyrite deposit, South Australia

J. GRAHAM

Division of Mineralogy, CSIRO
P. O. Wembley, Western Australia 6014

Abstract

Electron microprobe examination of a suite of samples from the Nairne pyrite formation (Shepard's Hill Quarry) has revealed two new minerals, a vanadiferous manganochromite, $(Mn,Fe)(Cr,V)_2O_4$, and a palladium diantimonide, $PdSb_2$, and has indicated several unusual occurrences including alabandite, graphite, and native nickel, suggestive of highly reducing conditions. The complex mineralogy of this sedimentary deposit is a result of a high-grade metamorphism and subsequent slight alteration.

Introduction

General studies of the Nairne pyrite ores at Brukunga, 47km east of Adelaide, South Australia, have been made by Skinner (1958), LaGanza (1959a), George (1967), and Nenke (1972). The pyrite member is found at the base of the Kanmantoo Group, which consists of at least 8000m of bedded, fine-grained quartzites, greywackes, and siltstones. The pyritic beds are of Cambrian age, and have been traced for 100km. This extension along the strike, together with the mineral relationships and laboratory evidence, strongly suggests a sedimentary origin, but considerable remobilization occurred during amphibole-facies metamorphism. Sulfur content is highly correlated with graphite. The latter varies from 1–2.4 percent in the ore beds, and these elements are thought to have a common biogenic origin (Nenke, 1972).

Major sulfides throughout the series consist of pyrite and hexagonal pyrrhotite, with chalcopyrite, galena, and sphalerite, less arsenopyrite, and some tetrahedrite associated with the galena. There is a complex arrangement of veins and jointing which affects the mineralogical associations. The most important veining set from a mineralogical point of view is that of the "tension gash veins" [George's (1967) nomenclature], which occur at right angles to the fold axis and the mineral lineation. The tension gash veins contain massive pyrrhotite and a range of sulfosalts and other unusual minerals.

George's work (1967, 1969a,b) concentrates largely on the origin and metamorphism of the ore body, and Nenke's (1972) on the major mineralogy of the tension gash veins. The present work describes some mineralogical features not previously discussed, some of which may have a bearing on theories of the history of the deposit.

Manganochromite—a new mineral

Description

In one polished section from the edge of a tension gash vein in ore body 1, several euhedral grains are present near the interface between massive pyrrhotite and gangue. Some are elongated, ranging in size from about 10μm diameter to about 80μm × 800μm (Fig. 1). The color in reflected light is brownish grey, isotropic, and more highly reflecting than chromite. A few grains are appreciably zoned as revealed by qualitative probe analysis, and each grain has a significantly different cation ratio from the others. Despite the large differences in composition (Table 1), reflectance and microhardness do not vary greatly. $VHN_{20g} = 1000 \pm 70$ (mean of 10 measurements covering several grains). For the grain corresponding to analysis 4, reflectances in air, measured against a calibrated secondary chromite standard, are: 470nm, 16.8 percent; 546nm, 16.5 percent; 589nm, 16.5 percent; 650nm, 16.3 percent. X-ray study shows the mineral to have the cubic spinel structure so that it is isomorphous with chromite, space group *Fd3m*. Manganochromite has a = 8.47A, $Z = 8(M_3O_4)$, G(calc) 4.86–4.90. The first eight lines (using a Gandolfi camera calibrated with ThO_2) are 4.89(111)w;

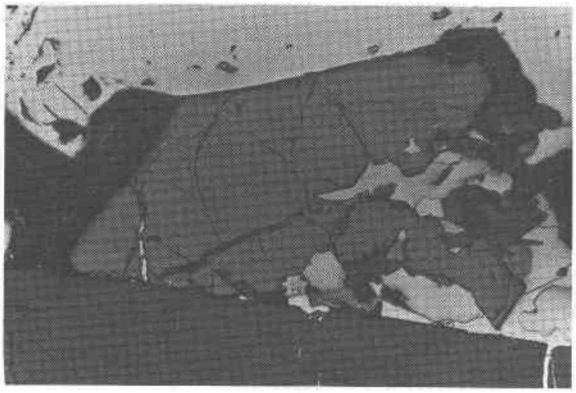

Fig. 1. A somewhat irregular manganochromite grain (pale grey) lying between hexagonal pyrrhotite (white) and a large diopside crystal (grey). Width of field 450μm.

2.99(022)w; 2.55(113)s; 2.44(222)w; 2.12(004)vw; 1.73(224)w; 1.63(115)s[1]; 1.50(044)s. Copper radiation was used, and to minimize fluorescence effects only the back surface of the film was developed. Synthetic $MnCr_2O_4$ described by Clark *et al.* (1931) has a = 8.453A.

Microprobe analyses were affected by the overlap of $K\alpha$ and β radiation from adjacent elements. Overlap parameters were determined from the pure metal standards for the actual spectrometer settings used. Starting with V, which needs no correction, the counts for Cr, Mn, and Fe were reduced by the appropriate fraction of the V, Cr, and Mn counts. The iron content was checked using Fe$K\beta$, with similar results. Matrix corrections were performed by Colby's Magic IV program, on-line to our MAC 400S microprobe analyzer.

An overall spinel composition was assumed, in which manganese was the predominant divalent metal and chromium the predominant trivalent metal; the name manganochromite (approved by the IMA Commission on New Minerals and Mineral Names) is given by analogy with the name magnesiochromite, $MgCr_2O_4$. Most of the grains analyzed show considerable substitution of vanadium for chromium, so that this occurrence is a highly vanadiferous variety.

The assumed chromite stoichiometry necessitates that Mn, Fe, and Zn are divalent and Cr and V are trivalent, except perhaps in analysis 1, where up to 40 percent of the iron could be in the trivalent state. The occurrence of divalent manganese and trivalent vanadium is consistent with evidence for reducing conditions described later. By comparison with synthetic $MnCr_2O_4$ and other chromium and vanadium spinels, manganochromite probably exhibits normal occupancy (Strunz, 1970, p. 176).

Long *et al.* (1963) noted two types of a manganese vanadate spinel from Outokumpu which extend our manganochromite compositions towards a vanadium end-member (Table 1, a and b). If the balance of their analysis is assigned to ZnO, good agreement with a spinel formula is obtained. As there is a deficit of divalent metals, there is also the possibility of some divalent vanadium or chromium.

Zoned Al-poor chromites from Outokumpu contain up to 4 percent MnO, 12 percent V_2O_3, and 9.6 percent ZnO (Weiser, 1967), but these elements are normally present only at low levels in natural chromites. The Al, Mg, and Ti contents of the Nairne chromites are below about 0.01 percent, except that up to 0.5 percent TiO_2 is observed near the boundary of contiguous rutile. One grain (Fig. 2) crystallized in pyrrhotite in conjunction with a rutile grain; small inclusions of pyrrhotite were trapped or precipitated along the boundary, and one of these can be seen in the photograph. The rutile contains 0.7 percent Cr, 0.25 percent V, 0.2 percent Mn, 0.4 percent Fe, and 0.5 percent W, the spinel probably being the source of the first three elements.

The rutile structure must have a high affinity for tungsten, as there is no obvious source for the tung-

Table 1. Microprobe analyses of manganochromite and a manganese vanadate spinel

	1	2	3	4	5	6	7	8	a	b
V_2O_3	1.7	9.9	12.3	13.4	15.1	17.9	21.3	27.6	53.0	63.3
Cr_2O_3	62.3	56.9	55.2	54.1	51.0	51.4	44.7	40.6	16.1	4.7
MnO	24.0	21.4	19.5	20.4	19.3	23.5	21.6	25.4	22.0	22.0
FeO	9.4	8.9	10.0	9.5	9.5	6.5	8.6	7.0	7.6	7.6
ZnO	1.7	1.8	2.2	2.2	2.3	0.6	1.3	0.6	(1.3)	(2.4)
Total	99.0	98.9	99.2	99.6	97.1	99.8	97.5	101.2	98.7	97.6

Atomic proportions on the basis of O = 4.

1. $(Mn_{0.77}Fe_{0.30}Zn_{0.05})_{1.12}(Cr_{1.88}V_{0.04})_{1.92}O_4$
2. $(Mn_{0.68}Fe_{0.28}Zn_{0.05})_{1.01}(Cr_{1.69}V_{0.30})_{1.99}O_4$
3. $(Mn_{0.62}Fe_{0.31}Zn_{0.06})_{0.99}(Cr_{1.64}V_{0.37})_{2.01}O_4$
4. $(Mn_{0.65}Fe_{0.30}Zn_{0.06})_{1.01}(Cr_{1.60}V_{0.40})_{2.00}O_4$
5. $(Mn_{0.62}Fe_{0.31}Zn_{0.08})_{1.01}(Cr_{1.52}V_{0.46})_{1.98}O_4$
6. $(Mn_{0.74}Fe_{0.20}Zn_{0.02})_{0.96}(Cr_{1.50}V_{0.53})_{2.03}O_4$
7. $(Mn_{0.70}Fe_{0.27}Zn_{0.04})_{1.01}(Cr_{1.35}V_{0.65})_{2.00}O_4$
8. $(Mn_{0.79}Fe_{0.22}Zn_{0.02})_{1.03}(Cr_{1.18}V_{0.81})_{1.99}O_4$

a. $(Mn_{.6}Fe_{.2}Zn_{.04})_{.9}(Cr_{.5}V_{1.6})_{2.1}O_4$
b. $(Mn_{.6}Fe_{.2}Zn_{.1})_{.9}(Cr_{.1}V_{1.9})_{2.0}O_4$

All chromite analyses also include from .03 to .40% sulfur.
Metal standards. Weight percent.
Analyses a and b are from Long et al. (1963).

---

[1] Obscured by ThO_2 line.

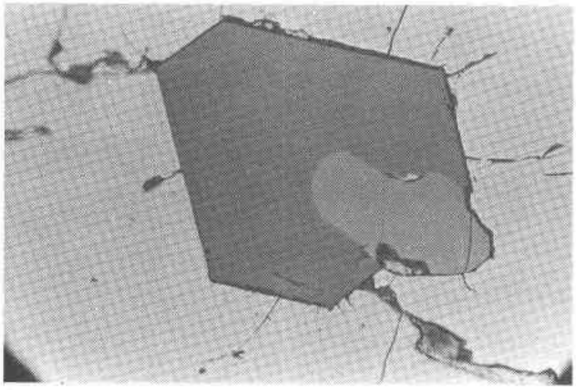

Fig. 2. A euhedral grain of manganochromite (dark grey) in a pyrrhotite matrix (white). The lighter grey tongue is rutile containing Cr, V, Mn, Fe, and W. Pyrrhotite inclusions occur along the boundary, only the largest of which is visible in the print. Width of field 220μm.

sten in the rutile of Figure 2, and no other tungsten-bearing minerals have been recognised (compare Graham and Morris, 1973).

Chemical associations

The spinel. The overall chromium and vanadium content of the deposit is about 200 ppm (Nenke, 1972). Manganese has concentrated into the spinel from an overall content of about 0.1 percent, despite the abundance of ferrous iron in the vicinity. The zinc content is also surprising, in view of the preference of zinc for the sulfide phase. Vanadium (overall concentration in the deposit about 100 ppm) must enter the spinel when the supply of chromium is restricted, because of the rather high octahedral stabilization energy of vanadium in the reduced trivalent form.

Katsura and Muan (1964) have already pointed out that the Fe/Cr ratio of a normal chromite varies with pO_2, and similar results are inferred for the Mg and Al content by Ulmer (1969) and Hamlyn (1975); the same may be true of the Mn content, and it seems likely that an experimental study of the spinel systems could give an understanding of pO_2–pS_2–T conditions during metamorphism or hydrothermal alteration.

Czamanske *et al.* (1976) have analyzed spinels from a layered gabbro which were also somewhat enriched in manganese and vanadium and were low in MgO and Al_2O_3. They are thought to have crystallized from a sulfide melt. Zoning in such spinels is very sharp (Ewers *et al.*, 1976), in contrast to the more subtle zoning in some of the manganochromite grains. The low concentrations of MgO and Al_2O_3 could be related to their low solubility in the sulfide phase. This would restrict their availability to the spinel if the sulfide is the source of the spinel, or if transport through the sulfide is involved in the spinel formation.

The shapes of the spinel grains and the enrichment in trace transition metals give some indication of the mobility involved in the metamorphic processes. Probe analyses of the spinels suggest that there may be some mutual solubility of oxide and sulfide, as contents up to 0.4 percent S have been obtained. The sulfur could be present as a submicroscopic sulfide dispersion, but it is not a spurious reading due to secondary emission or multiple scattering. The readings are unaffected when surrounding sulfides are covered with ink filled with a heavy absorber, and they do not rise systematically as the edge of the grain is approached. Moreover, such counts are not found in quartz grains similarly surrounded by sulfide. Sulfur contents of the less regular grains at the boundary of the gangue are lower, of the order of 0.05–0.08 percent, and these grains may not have been mobilized as freely during metamorphism. Solubility of oxygen in solid pyrrhotite has already been deduced for a natural occurrence (Bennett *et al.*, 1972), and a similar distribution of lamellar magnetite has been observed in the synthetic sample described by Ewers *et al.* (1976), in addition to the euhedral chromite and magnetite which crystallized during solidification. On the other hand, the metamorphic mobility of the sulfide phase is well known, and penetration of sulfides into cracks in the silicate and oxide phases can be seen in Figure 1.

Transport of the metals through the solid sulfide at metamorphic temperature is no problem—Ni, Cu, Co, and Fe have been shown to diffuse macroscopic distances in a few hours at low temperatures, especially if water is present (Ewers, 1972). For example, Ni under a relatively small chemical gradient moved about 1mm into pyrrhotite in 200 hours at 400°C in dry conditions. With a larger Ni gradient, in aqueous conditions, the alteration front moved 0.23mm in 1 hour at 241°C.

Data are not so easy to obtain for Cr diffusion, because chromic solutions are strongly oxidizing and highly reactive, and chromous solutions are difficult to prepare and standardize. However, we were able to show that Cr diffuses moderately rapidly at 500°C in dry conditions, by annealing pyrrhotite in contact with Cr powder freshly reduced with hydrogen. The Cr concentration in the pyrrhotite never exceeded 0.5 percent, but levels of 0.04 percent were present at a depth of 40μ within a grain of pyrrhotite after 150 hours at 500°C. Although apparently an order of magnitude slower than for Ni, this diffusion rate is very fast where a geological time-scale is involved. A solid-state diffusion mechanism for the formation of the spinel is therefore feasible.

It should be remembered that manganochromite occurs in contact with massive sulfide.

Cr and V in other minerals. No Cr or V minerals have previously been observed at Nairne. In the present work these elements have been found in the spinel phase, in rutile, and in a few grains of silicate minerals at the boundary between the massive sulfide and the gangue. Complete equilibrium has not been attained, since there is often a strong compositional gradient in what appears to be a single mineral grain. The concentration of Cr, V, and Mn decrease away from the sulfide boundary. The Cr and V may have been concentrated from the sulfide phase or from solutions which would have been drawn to the site of the vein in the same way as the sulfides.

Two microprobe analyses of chlorite crystals gave a structural formula approximating $(K_{0.04}Mg_{7.91}Fe_{0.70}Mn_{0.13}Cr_{0.65}V_{0.15}Al_{2.17})(Al_{2.41}Si_{5.59})O_{20}(OH)_{16}$. This material contains 4.0–4.5 percent Cr_2O_3 and approximately 1 percent V_2O_3 and MnO, and can be classified as kämmererite. Two analyses of an amphibole gave a formula $(Ca,K)_{2.06}[(Mg,Mn,Fe)_{3.83}(V,Cr,Al)_{1.24}](Al_{1.46}Si_{6.54})O_{22}(OH)_2$, with 5 percent V_2O_3, 4.2 percent Cr_2O_3, and 0.9 percent Mn. This can be classified as a vanadiferous chromian hornblende.

Two different micas contained 2.2–4.3 percent V_2O_3, 3.7–6.1 percent Cr_2O_3, and 0.2–1.3 percent MnO. Average compositions would be represented by the formulae $K_{1.54}[(Mg,Fe,Mn)_{1.67}(Al,Cr,V)_{3.00}](Al_{1.88}Si_{6.12})O_{20}(OH)_4$ (with very low Fe,Mn) and $K_{1.30}[(Mg,Fe,Mn)_{4.35}(Al,Cr,V,Ti)_{1.52}](Al_{2.52}Si_{5.48})O_{20}(OH)_4$.

The former is closer to a dioctahedral (muscovite) and the latter to a trioctahedral (phlogopite) composition. This confirms George's (1967) observation that there must be a trioctahedral mica present, whereas Skinner (1958) reported only muscovite.

Manganese in other minerals. Manganese occurs in sphalerite at Nairne (Skinner, 1958). My analyses indicate ~7.5 percent Mn compared with Skinner's value of 2.5 percent, and the higher value agrees better with overall sulfide compositions obtained by Nenke (1972). The Nairne sphalerite contains ~11 percent Fe, and when present in quantity it is associated with chalcopyrite. I have also found a number of other manganese minerals. Alabandite is present in appreciable amounts in sulfides from the tension gash veins, and nearly always appears in association with chalcopyrite. Nenke has demonstrated that not all the Mn occurs in sulfide minerals. I have found considerable Mn contents in the spinel and layer silicate phases, but only at boundaries of gangue and massive pyrrhotite. In other areas of the ore bodies, spessartine has been observed, and the grain size may be very large. A number of grains of pyrophanite have been observed adjacent to rutile from No. 2 ore body, and a manganiferous siderite occurs sporadically. It is not easy to guess at the distribution of Mn prior to metamorphism, but the manganochromite and layer-silicates indicate considerable rearrangement.

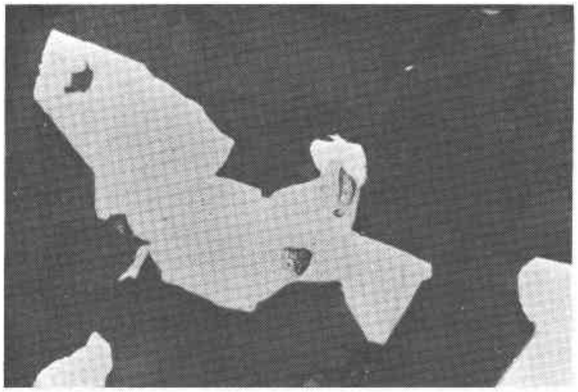

Fig. 3. Small grain of palladium diantimonide (white) in contact with chalcopyrite (light grey). Width of field 143μm.

Palladium antimonide, $PdSb_2$

A small grain of chalcopyrite within the gangue in the same polished section that contained the manganochromite had a highly reflecting appendage (Fig. 3), approximately 13 × 6μm. A microprobe analysis of this grain is given in Table 2, which shows that the composition is very close to $PdSb_2$. It was not possible to obtain an X-ray diffraction pattern, but the mineral is optically isotropic in this section. A pyramid hardness indentation partly in the mineral and partly in the chalcopyrite indicates a VHN_{10g} of about 260, slightly higher than for chalcopyrite. The mineral itself probably has a slightly higher value still, but there is no polishing relief against chalcopy-

Table 2. Microprobe analysis of palladium antimonide mineral

Element	Weight %	Atomic %
Pd	31.30	33.9
Sb	67.44	63.8
Fe	0.64	1.3
Cu	0.54	1.0

Structural formula $Pd_{1.0}(Sb_{1.9}Fe_{.04}Cu_{.03})_{2.0}$

Metal standards.

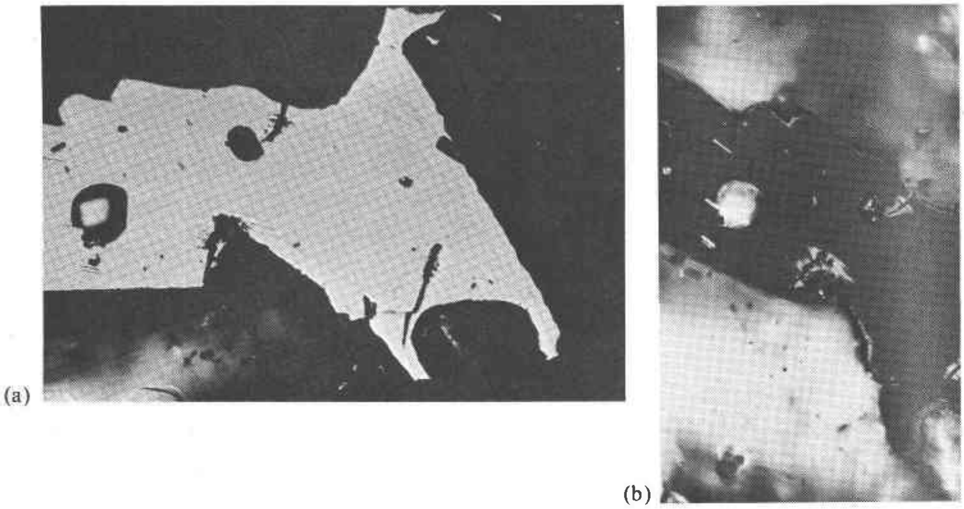

Fig. 4. (a) A grain of pyrrhotite isolated in silicate gangue, hexagonal with monoclinic margins. The view (b) under crossed nicols shows graphite laths (white) and evidence of alteration about several defects in the grain. Width of field 200μm, oil.

rite. Color is white, and reflectivity measured against a calibrated pyrite secondary standard is 55.4 percent at 470nm, 53.6 percent at 546nm, and 56.6 percent at 589nm and 650nm.

Synthetic $PdSb_2$ has the pyrite structure (Raub *et al.*, 1963) and since the new mineral is isotropic, it may also have this structure.

Many other compounds of the platinoids with the pyrite structure have been made synthetically (Hulliger, 1968) and some are known as minerals, including geversite ($PtSb_2$), sperrylite ($PtAs_2$), and michenerite (PdBiTe). It is probable that borishanskite (PdAsPb) also has this structure. The latter mineral was described by Rasin *et al.* (1975), who assigned it the orthorhombic α-PdBi structure. However, the atom ratios are wrong for this structure. All but two of its powder diffraction lines can be well-indexed assuming a cubic pyrite structure, cell size a = 5.19A, and on the basis of its AB_2 stoichiometry, this is the preferred interpretation. An admixture of α-PdBi or perhaps PdAs may explain the extra lines. Of the above minerals, the hardness values of geversite and michenerite and the reflectivities of sperrylite, michenerite, and borishanskite are similar to those of our new mineral; the reflectivity of geversite is reported to be higher. These similarities tend to confirm the pyrite structure of the new mineral.

Pyrrhotite

Oxidation-produced monoclinic pyrrhotite and pyrite

George (1967) stated that some of the disseminated pyrrhotite was monoclinic, and I have confirmed this with a magnetic colloid suspension, assuming that strongly magnetic material is monoclinic. Small grains are entirely monoclinic and larger grains are hexagonal with a 5–10μm monoclinic rim. A typical grain with monoclinic rim is shown in Figure 4a. Even the massive hexagonal pyrrhotite from the tension gash veins has narrow monoclinic margins which extend along many of the cracks in the pyrrhotite. These monoclinic rims are always present in the neighborhood of pyrite inclusions, and nowhere was a pyrite–hexagonal pyrrhotite interface observed. Isolated pyrite grains within massive pyrrhotite are also often separated from pyrrhotite by shrinkage voids similar to those produced when pyrite is formed by hydrothermal leaching of iron from pyrrhotite with or without nickel–iron exchange (Ewers, 1972). It seems certain that the monoclinic rims are the result of late oxidation of hexagonal pyrrhotite, a process which may proceed as far as the formation of pyrite, since I have observed pyrite pseudomorphs after pyrrhotite, a type of pyrite occurrence which was not observed by LaGanza (1959a,b). It is surrounded by "concentric FeS_2" in the same way as LaGanza's "box work pyrite", but in this case both the massive pyrite and the "concentric FeS_2" may be rimmed by "zoned pyrite".

The apparent ease with which small hexagonal pyrrhotite grains are oxidized to the monoclinic form despite their silicate surroundings suggests an electronic oxidation process similar to the deep supergene alteration of the sulfide nickel ore bodies at Kambalda, Western Australia (Thornber, 1975). By electrical measurement a high degree of connectivity has been demonstrated, as at Kambalda, between apparently isolated sulfide grains in polished sections from Nairne. It seems unlikely, however, that electrical contact is maintained to the smallest sulfide "particles" by comparison with Kambalda, where grains entirely surrounded by silicates in the truly disseminated zone are protected from oxidation. An alternative explanation is given below. The net result of the oxidation would be the movement of small amounts of metal ions into the surrounding silicates or ground waters.

Lamellar graphite

As shown in Figure 4b, graphite lamellae are present within the pyrrhotite grains, and their orientation seems to be crystallographically controlled. It has been assumed by Marx (1971, 1972) that graphite can be formed from CO_2 or CO by the reducing effect of pyrrhotite. Occurrence of the graphite within the pyrrhotite suggests to me that the two minerals in this case are syngenetic, in agreement with Nenke (1972). Is it possible that the highly reducing conditions at the time of crystallization indicated by the graphite explain the absence of primary monoclinic pyrrhotite? Thus, reducing conditions may cause the formation of more reduced pyrrhotite phases from the expected monoclinic variety by altering the oxidation state of either the metal or the sulfur component. Occurrences of primary hexagonal pyrrhotite/pyrite occur in graphitic schists in the Malé Karpaty Mountains (Kantor and Durkovicova, 1973), where alabandite also occurs (Kantor and Kristin, 1973). In fact graphite and hexagonal pyrrhotite–pyrite seem to be commonly associated.

An unexpected piece of evidence from Nairne pointing to highly saline conditions, probably during metamorphism, is the occurrence of an inclusion of halite in a pyrrhotite grain from ore body 3.

Nickel

The overall Ni content of the Nairne pyrite deposit rarely exceeds 100 ppm, and is highly correlated with sulfur (Nenke, 1972). Nickel minerals previously observed are ullmannite and breithauptite, but I have observed a very curious distribution of minute particles of nickeline, pentlandite, and "native nickel" near pyrrhotite grains at several places in the ore bodies. These grains are rarely more than about 1μm in diameter, and it was at first thought that the "native nickel" must be due to contamination during sectioning. However, the material continued to be observed after new sections were prepared in various ways and even when a sample was prepared in an independent laboratory. It occurs in the form of highly reflecting small particles much whiter than nearby pyrrhotite and pyrite, usually in a matrix of mica a few microns from the mica–pyrrhotite interface. "Native nickel" is much more common than nickeline and pentlandite, and although the particles are too small for accurate microprobe analysis, it is clear that the Fe content is lower than that of the more usual awaruite. The Ni figure is at least 88 percent Ni and probably more, and Fe counts are very low (~5.5 percent). A typical occurrence is shown in Figure 5.

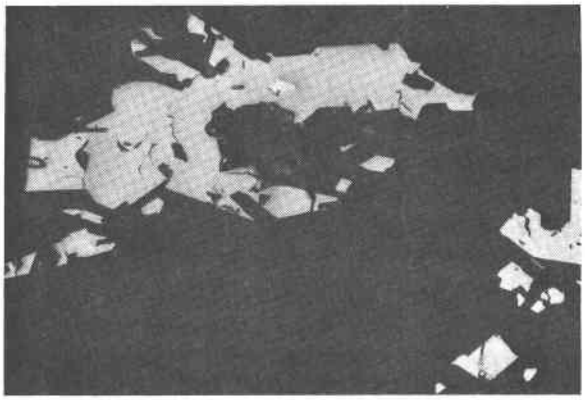
Fig. 5. Typical mode of occurrence of native nickel. Blebs of pyrrhotite and native nickel (more highly reflecting) in mica, lining edges of embayment in a pyrrhotite grain (light grey). The large white grain in pyrrhotite is chalcopyrite. Width of field 180μm. Oil immersion. The largest fragment here is ~4μm × 2μm.

It is known that Ni as Ni^{2+} is easily absorbed by iron sulfides at temperatures even down to ambient (Ewers, 1972), and the observation of native nickel so close to nickel-free pyrrhotite appears to be anomalous, especially in view of the stability of NiS. This is obviously a non-equilibrium situation, and the few microns of mica must be an effective shield between the nickel and the pyrrhotite. The oxidation of hexagonal to monoclinic pyrrhotite is taking place in very different solutions to those of the nickel-rich Perseverance deposit described by Nickel *et al.* (1977), and, if anything, our monoclinic rims are depleted in nickel instead of enriched, although the microprobe evidence is inconclusive on this point. No satisfactory explanation of these phenomena can be offered. One could perhaps suggest quite unusual Eh/pH conditions, and some support might be found in the relevant Pourbaix diagram (Cowan and Staehle, 1971), which shows that if the pH is high enough, Ni is soluble as the ion $HNiO_2^-$ (Fig. 6), while Fe is still

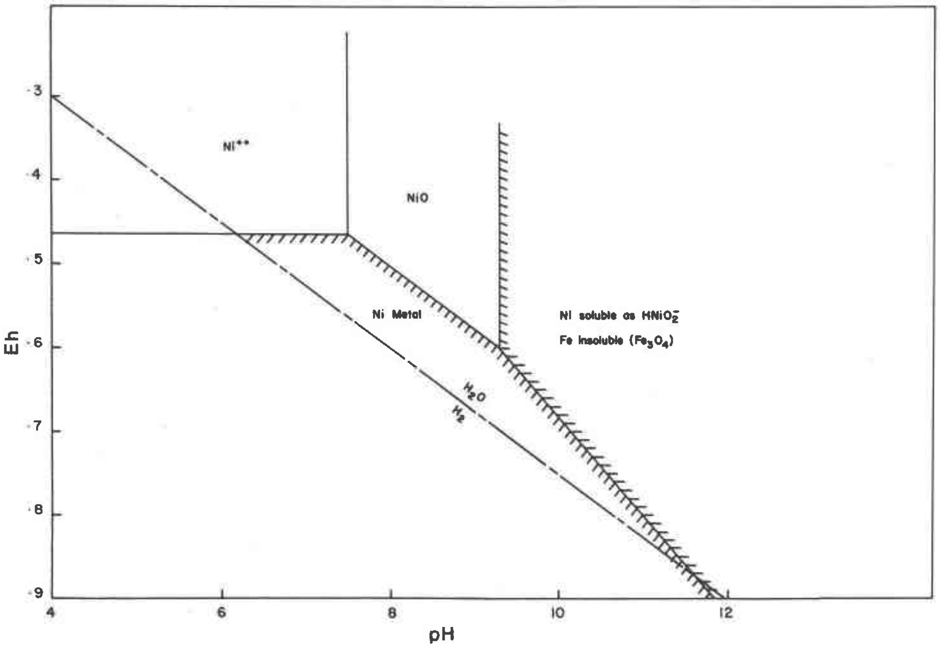

Fig. 6. Eh–pH diagrams for nickel–H_2O system at 100°C, drawn for a concentration of 10^{-6} dissolved species (Cowan and Staehle, 1971). Sulfide concentration is negligible. The relevant regions of stability of metallic nickel and of soluble nickel are outlined.

insoluble. An idealized equation would be

$$8(Fe,Ni)_9S_{10} + 6OH^- \rightleftarrows 10Fe_7S_8 + 2HNiO_2^- + 2H_2O + 4e^-$$

If the nickel solution moves to a region in the silicates where the pH is lower (movement to the left from the $HNiO_2^-$ region in Fig. 6), there is the possibility of reprecipitation of the nickel according to the equation $2e^- + 3H^+ + HNiO_2^- \rightleftarrows Ni + 2H_2O$.

It will be noticed that the oxidation of the pyrrhotite to Fe_7S_8 and the reduction of the nickel to nickel metal has taken place without external electron transfer. The proposed mechanism is therefore capable of explaining the oxidation of pyrrhotite grains isolated in the silicate matrix, as well as the occurrence of adjacent native nickel. The monoclinic rims could then be produced by an increase in pH without necessarily involving a change in Eh. This is not, however, a possible origin for the secondary pyrite unless the original nickel content of the deposit was quite high. The difficulty with this explanation is the low sulfur activity required, but it seems obvious from the occasional occurrence (in the same section) of the nickel minerals previously referred to and the common occurrence of pyrrhotite in similar situations that the local conditions for the formation of the native nickel are critical.

M. Bussell (personal communication, 1972), in two experiments on the dehydration of samples of serpentine nickel ore, found a very nickel-rich nickel–iron phase among the products (90 percent Ni and 95 percent Ni respectively), which could be due to similar reactions. Unfortunately he was not able to repeat the results, another indication that conditions in the solution are critical.

The proposed mechanism contrasts with reduction mechanisms during serpentinization which have been proposed for the formation of awaruite and josephinite (*e.g.*, Botto and Morrison, 1976). Such reduction mechanisms do not explain why the nickel grains only occur near sulfide boundaries.

Other minerals present

In the course of this work many small grains were qualitatively studied under the microprobe in the hope that they might throw some light on the origin of this unusual ore body. Little emphasis was placed on the gangue minerals, but a few interesting observations were made on them.

For example, four kinds of phosphates have been observed in our polished sections, sometimes included in pyrrhotite and sometimes in the silicates. Two of them are widespread, a chlorapatite and another without chlorine which is presumably a hydroxy- or fluorapatite. The third and fourth are rare-earth phosphates of complex composition. The third

Table 3. Minerals observed at Nairne

		Ore minerals			
hexagonal pyrrhotite	Fe_9S_{10}	arsenopyrite	$FeAsS$	breithauptite	$NiSb$
monoclinic pyrrhotite	Fe_7S_8	boulangerite	$Pb_5Sb_4S_{11}$	gudmundite	$FeSbS$
pyrite (several generations)	FeS_2	stannite	Cu_2SnFeS_4	cubanite	$CuFe_2S_3$
marcasite	FeS_2	freibergite	$(Cu,Fe,Ag)_{12}Sb_4S_{13}$	native nickel	Ni(Fe?)
galena	PbS	graphite	C	pentlandite	$(Fe,Ni)_9S_8$
sphalerite (with Fe,Mn)	ZnS	pyrargyrite	Ag_3SbS_3	nickeline	$NiAs$
chalcopyrite	$CuFeS_2$	ullmannite	$NiSbS$	palladium antimonide	$PdSb_2$
alabandite	MnS				
		Miscellaneous non-silicates			
rutile	TiO_2	apatite	(two kinds)	manganoan siderite	$(Fe,Mn)CO_3$
pyrophanite	$MnTiO_3$	rare earth phosphates	(two kinds)	halite	$NaCl$
manganochromite (with Fe,V)	$MnCr_2O_4$	calcite	$CaCO_3$		
		Silicates			
quartz		amphiboles*		diopside	
dioctahedral micas*†		chlorites*		titanite	
trioctahedral micas*†		feldspars†		garnet	
andalusite		zircon		prehnite	
kyanite		spessartite		tremolite	
sillimanite		scapolite		other aluminosilicates	

* *May contain Mn, V, Cr.*
† *May contain Ca, Mg, Ba, Ti.*

contains appreciable amounts of Ca, Th, Ce, and Nd, lesser La and Pr, and minor Sm and Gd, and is included in pyrrhotite grains. The fourth contains all the lanthanides of atomic numbers 57–65 (excluding Pm) but not Ca or Th. Only one grain was observed, but it was comparatively large (~30μm). The distribution of the minute blebs of the third phosphate was reminiscent of that found in iron ore from the Brockman Iron Formation (Graham, 1973), where also a second phosphate of much larger size was found. Different combinations of rare-earth elements evidently favor different "crystallizing forces"; this could be due to different ratios of surface/internal energy, resulting in small particle sizes for some combinations and large individual particles for others. Alternatively kinetic factors during mobilization may be responsible, or the different compositions and distributions of phosphate may represent different generations.

There is also a variety of potassium-containing silicates, many different kinds appearing as inclusions in pyrite and other minerals. Hyalophane, for example, occurs both in the gangue and as inclusions in pyrite, and there appear to be at least two different barium-containing micas. Two different potassium aluminum silicates contain appreciable amounts of titanium, and it would take a great deal of work to fully understand the silicate relationships. Minerals observed at Nairne are listed in Table 3.

The variety of compositions of the manganochromites and the non-uniform distribution of Mn,V,Cr over short distances in particular silicate minerals argue that equilibrium was not attained during metamorphism. The alteration of hexagonal pyrrhotite to the monoclinic variety and to various generations of pyrite, and especially the occurrence of native nickel, are indications of supergene processes. The metamorphism has been responsible for concentrating the trace elements and for the formation of many of the unusual minerals at Nairne; it is not yet clear how great an effect the subsequent alteration has had on the major mineral assemblages.

Acknowledgments

The author is indebted to Dr. J. Stephens and Dr. R. A. Both for specimens carefully collected from the Shepard Hill quarry.

References

Bennett, C. E. G., J. Graham and M. R. Thornber (1972) New observations on natural pyrrhotites: II. Lamellar magnetite in monoclinic pyrrhotite. *Am. Mineral., 57,* 1876–1880.

Botto, R. I. and G. H. Morrison (1976) Josephinite: a unique nickel-iron. *Am. J. Sci., 276,* 241–274.

Clark, G. L., A. Ally and A. E. Badger (1931) The lattice dimensions of spinels. *Am. J. Sci., 22,* 539–546.

Cowan, R. L. and R. W. Staehle (1971) The thermodynamics and electrode kinetic behaviour of nickel in acid solution in the temperature range 25°–300°C. *J. Electrochem. Soc., 118,* 557–568.

Czamanske, G. K., G. R. Himmelberg and F. E. Goff (1976) Zoned Cr, Fe-spinel from the La Perouse layered gabbro, Fairweather Range, Alaska. *Earth Planet. Sci. Lett., 33,* 111–118.

Ewers, W. E. (1972) Nickel–iron exchange in pyrrhotite. *Proc. Australasian Inst. Min. Metall., 241,* 19–26.

———, J. Graham, D. R. Hudson and J. Rolls (1976) Crystallization of chromite from nickel–iron sulphide melts. *Contrib. Mineral. Petrol., 54,* 61–64.

George, R. J. (1967). *Metamorphism of the Nairne Pyrite Deposit.* Ph.D. Thesis, University of Adelaide.

——— (1969a) Sulphide–silicate reactions during metamorphism of the Nairne Pyrite Deposit. *Proc. Australasian Inst. Min. Metall., 230,* 1–9.

——— (1969b) Sulphide vein formation during metamorphism of the Nairne Pyrite Deposit. *Proc. Australasian Inst. Min. Metall., 230,* 9–19.

Graham, J. (1973) Phosphorus in iron ore from the Hamersley Iron Formation. *Proc. Australasian Inst. Min. Metall., 246,* 41–42.

——— and R. C. Morris (1973) Tungsten- and antimony-substituted rutile. *Mineral. Mag., 39,* 470–473.

Hamlyn, P. R. (1975) Chromite alteration in the Panton Sill, East Kimberley Region, Western Australia. *Mineral. Mag., 40,* 181–192.

Hulliger, F. (1968) Crystal chemistry of the chalcogenides and pnictides of the transition elements. *Structure and Bonding (4),* 83–229.

Kantor, J. and J. Durkovicova (1973) Structural modifications of pyrrhotite at pyrite–pyrrhotite deposits of the Malé Kaparty Mts. *Geologicky Zbornik-Geologica Carpathica XXIV, 2, Bratislava, Nov.,* 231–246.

——— and J. Kristin (1973) Alabandite from the metamorphosed pyrrhotite-pyrite deposit of Helpa in the Nizke Tatry Mts. *Geologicky Zbornik-Geologica Carpathica XXIV, 2, Bratislava, Nov.,* 247–253.

Katsura, T. and A. Muan (1964) Experimental study of equilibria in the system FeO–MgO–Cr_2O_3 at 1300°C. *Trans. Met. Soc. AIME, 230,* 77–84.

LaGanza, R. F. (1959a) *The Nairne sulphide deposit.* M.Sc. Thesis, University of Adelaide.

——— (1959b) Pyrite investigations at Nairne, South Australia. *Econ. Geol., 54,* 895–902.

Long, J. V. P., Y. Vuorelaimen and O. Kouvo (1963) Karelianite, a new vanadium mineral. *Am. Mineral., 48,* 33–41.

Marx, P. C. (1971) On the electrochemical origin of natural graphite. *Am. Mineral., 56,* 336–338.

——— (1972) Pyrrhotine and the origin of terrestrial diamonds. *Mineral. Mag., 38,* 636–638.

Nenke, J. A. (1972) *Geochemistry and mineragraphy of the Nairne Pyrite Deposit, Brukunga, South Australia.* Honours Thesis in Geology, University of Adelaide.

Nickel, E. H., P. D. Allchurch, M. G. Mason and J. R. Wilmshurst (1977) Supergene alteration at the Perseverance nickel deposit, Agnew, Western Australia. *Econ. Geol., 72,* 184–203.

Rasin, L. V., L. S. Dubakina, V. I. Meshchankina and V. D. Begizov (1975) Borishanskite—a new lead arsenide of palladium from the copper–nickel ores of the Talnakh differentiated intrusive. *Zap. Vses. Mineral. Obshch., 104,* 57–61 (*Am. Mineral., 61,* 502, 1976).

Raub, Ch. J., W. H. Zachariasen, T. H. Geballe and B. T. Matthias (1963) Super-conductivity of some new platinum metal compounds. *J. Phys. Chem. Solids, 24,* 1093–1100.

Skinner, B. J. (1958) The geology and metamorphism of the Nairne pyritic formation. *Econ. Geol., 53,* 546–562.

Strunz, H. (1970) *Mineralogische Tabellen.* Akademische Verlagsgesellschaft, Leipzig.

Thornber, M. R. (1975) Supergene alteration of sulphides I. A chemical model based on massive nickel sulphide deposits at Kambalda, Western Australia. *Chem. Geol., 15,* 1–14.

Ulmer, G. C. (1969) Experimental investigation of chromite spinels. In H.D.B. Wilson, Ed., *Magmatic Ore Deposits. Econ. Geol. Monograph No. 4.*

Weiser, T. (1967) Zinc- and vanadium-bearing chromites from Outokumpu, Finland. *Neues Jahrb. Mineral. Monatsh.,* 234–243.

Manuscript received, November 26, 1976; accepted for publication, April 14, 1978.